Available online at www.sciencedirect.com
SCIENCE DIRECT®
International Journal of Mass Spectrometry 232 (2004) 9–15
International Journal of Mass Spectrometry
www.elsevier.com/locate/ijms

Kinetics, thermodynamics, and ab initio calculations of $HS_2O_7^-(H_2SO_4)_x$ ($x = 1$–3) cluster ions☆

Stefan Rosén[a,b], Karl D. Froyd[a,b], Joachim Curtius[a,b,1], Edward R. Lovejoy[a,*]

[a] *NOAA Aeronomy Laboratory, 325 Broadway, Boulder, CO 80305, USA*
[b] *Cooperative Institute for Research in Environmental Sciences (CIRES), University of Colorado, Boulder, CO 80309, USA*

Received 23 September 2003; accepted 29 October 2003

Abstract

Temperature and pressure dependent decomposition kinetics of $HS_2O_7^-(H_2SO_4)_x$ ($x = 1$–3) cluster ions were measured in a quadrupole ion trap mass spectrometer. The kinetic data were analyzed with a master equation model to obtain the decomposition energies and energy transfer parameters for channels leading to elimination of sulfur trioxide and in some cases sulfuric acid. The ion cluster structures, vibrational frequencies and bond enthalpies were calculated ab initio at the HF/6-31+G(d) level of theory. The calculated bond energies agree well with the experimental results.

Keywords: Cluster ions thermodynamics; Sulfur trioxide; Sulfuric acid; Pyrosulfuric acid

1. Introduction

Cluster ions of the form $HS_2O_7^-(H_2SO_4)_x$ have been detected in the stratosphere [1], and have been used to infer limits on stratospheric SO_3 concentrations [2]. Laboratory studies by Arnold et al. indicate that SO_3 bonds strongly to $HSO_4^-(H_2SO_4)_x$ and that the kinetics of SO_3 clustering to $HSO_4^-(H_2SO_4)_x$ are near the high-pressure limit [3] in 0.38 Torr of He. However, the absolute stabilities of these clusters are unknown. Accurate knowledge of the cluster stabilities would significantly reduce the uncertainty in the derived stratospheric SO_3 concentrations. We have measured rate coefficients for the thermal decomposition of $HS_2O_7^-(H_2SO_4)_x$ ion clusters ($x = 1$–3) as a function of pressure (0.05–4 mTorr He) and temperature (303–433 K) in a quadrupole ion trap. Decomposition channels leading to elimination of sulfuric acid and sulfur trioxide are observed. The kinetic data were analyzed with a master equation model to obtain the decomposition energies. Ab initio calculations (HF/6-31+G(d)) of the cluster ion geometries, vibrational frequencies, and energies were also performed.

2. Experiment

2.1. Part I: decomposition

The kinetics of $HS_2O_7^-(H_2SO_4)_x$ ($x = 1$–3) cluster ions were studied with a flow reactor ion source coupled to an ion trap mass spectrometer. This experimental setup has been described previously [4]. H_2SO_4 vapor was generated by flowing about 15 STP $cm^3\,s^{-1}$ (STP = 273 K and 760 Torr) of Helium over hot (60 °C) liquid concentrated H_2SO_4 held in a stainless steel reservoir. The H_2SO_4 vapor was added to a total flow of about 110 STP $cm^3\,s^{-1}$ of Helium in the flow reactor and reacted with electrons produced upstream by a hot Iridium filament. The pressure in the flow reactor was typically about 0.9 Torr. The main negative cluster ions produced were $HSO_4^-(H_2SO_4)_x$ ($x \leq 5$) with a few percent of $HS_2O_7^-(H_2SO_4)_x$. SO_3 has an appreciable vapor pressure over the hot H_2SO_4 liquid, and presumably the SO_3 clusters are produced by SO_3 reaction with the $HSO_4^-(H_2SO_4)_x$ clusters. To enhance the signals of the larger clusters ($x \geq 2$), the pressure in the flow reactor was increased to about

☆ Supplementary data associated with this article can be found, in the online version, at doi:10.1016/j.ijms.2003.10.004.

* Corresponding author. Tel.: +1-303-497-5818; fax: +1-303-497-5822.
E-mail addresses: srosen@al.noaa.gov (S. Rosén), nlovejoy@al.noaa.gov (E.R. Lovejoy).
[1] Present address: Institute for Atmospheric Physics, Becherweg 21, University of Mainz, 55099 Mainz, Germany.

1387-3806/$ – see front matter © 2003 Published by Elsevier B.V.
doi:10.1016/j.ijms.2003.10.004

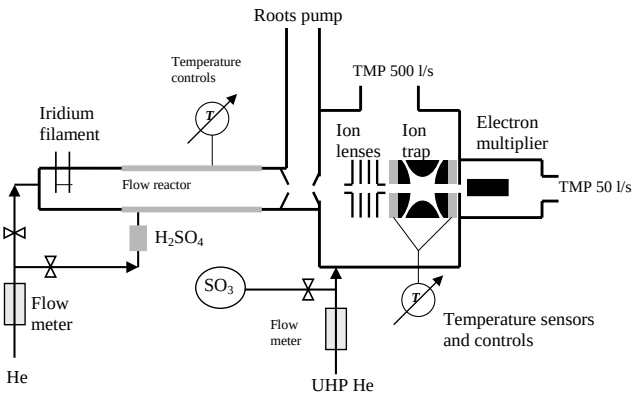

Fig. 1. Experimental set-up. Flow reactor ion source coupled to an ion trap mass spectrometer.

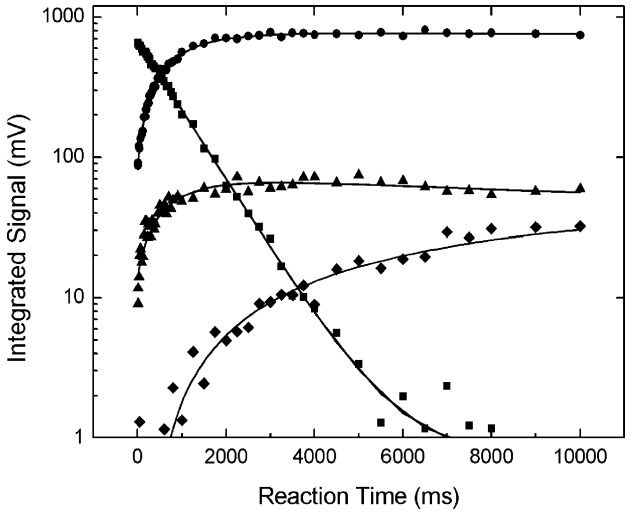

Fig. 2. Thermal decomposition (T = 312 K and P = 0.42 mTorr) of $HS_2O_7^-(H_2SO_4)_2$ cluster ion (mass 373, (■)) to yield $HSO_4^-(H_2SO_4)_2$ (mass 293, (●)) and $HS_2O_7^-(H_2SO_4)$ (mass 275, (▲)). The subsequent decomposition of $HS_2O_7^-H_2SO_4$ to $HSO_4^-H_2SO_4$ (mass 195, (◆)) is observed at longer times. Fits to the data are shown as solid lines.

4 Torr. Ions were sampled through a 0.25 mm aperture at the downstream end of the reactor, and focused into the ion trap by a set of four electrostatic lenses. The voltage on the first lens was controlled to gate ions into the trap. The experimental setup is shown in Fig. 1.

The experimental scheme used to measure the kinetics of thermal decomposition was as follows. Ions were accumulated for a fixed period of time (typically 10–100 ms), and a single mass was selected by applying a filtered noise field (FNF) across the endcaps [5]. Following accumulation, the ions were held in the trap for a variable reaction time, then scanned out of the trap to generate a mass spectrum. Kinetics were measured by monitoring the reactant and product ion signals as a function of the reaction time. First order decomposition rate coefficients were derived from the exponential decay of the signal as a function of reaction time. The first order rate constants were measured for different pressures (0.05–4 mTorr) and temperatures (303–433 K). Varying the flow of UHP He into the trap chamber controlled the pressure in the trap. The flow from the ion source reactor constituted from 4 to 14% of the total flow into the ion trap chamber. Fig. 2 shows an example of a measurement of the decomposition of the $HS_2O_7^-(H_2SO_4)_2$ ion cluster (mass 373) and the appearance of the two fragments $HSO_4^-(H_2SO_4)_2$ (mass 293) and $HS_2O_7^-(H_2SO_4)$ (mass 275). The subsequent decomposition of $HS_2O_7^-H_2SO_4$ to $HSO_4^-H_2SO_4$ (mass 195) is also observed.

2.2. Part II: ligand switching

The kinetics of the bimolecular ligand switching reaction

$$HSO_4^-(H_2SO_4)_2 + SO_3 \rightarrow HS_2O_7^-H_2SO_4 + H_2SO_4 \quad (1)$$

were also measured in the ion trap. $HSO_4^-(H_2SO_4)_2$ was selectively trapped and SO_3 was added directly to the ion trap chamber with the main Helium flow. The SO_3 vapour was drawn from a reservoir of solid SO_3 and passed through a heated needle valve into the main ion trap Helium flow. The SO_3 concentration was measured by monitoring the decay of SF_6^- in the ion trap and using a rate coefficient of 1.1×10^{-9} cm^3 per molecule per second for the reaction [3]

$$SF_6^- + SO_3 \rightarrow FSO_3^- + SF_5 \quad (2)$$

SF_6^- was generated in the ion source reactor by adding SF_6 downstream of the iridium filament. The ligand switching kinetics (reaction (1)) were measured at a constant trap pressure of 0.5 mTorr He and for a range of SO_3 concentrations (1×10^8 to 3×10^{10} molecule cm^{-3}) and temperatures (303–453 K).

2.3. Analysis of the data

Cluster bond energies were derived from a master equation analysis of the thermal decomposition kinetics, as described previously [6]. The thermal decomposition kinetics are described by the following equation:

$$\frac{d[i]}{dt} = z[\mathrm{He}]\sum_{j=1}^{\infty} P_{i,j}[j] - z[\mathrm{He}][i]\sum_{j=1}^{\infty} P_{j,i} - k_{\mathrm{uni},i}[i] \quad (3)$$

where z is the second-order collision rate constant for the bath gas He + reactant [7], and $P_{i,j}$ is the probability that a collision between the reactant and the bath gas changes the internal energy of the reactant from state j to state i. Collision transition probabilities were calculated with an exponential energy up model [6]. $k_{\mathrm{uni},i}$ is the first-order unimolecular decomposition rate constant of state i. Input parameters to the model are the bond energy E_0, the He/ion energy transfer parameter β, and the ab initio vibrational frequencies and rotational constants. Experimental data and the best fit master equation predictions for the reaction

$$HS_2O_7^-H_2SO_4 + He \rightarrow HSO_4^-H_2SO_4 + SO_3 + He \quad (4)$$

are shown in Fig. 3.

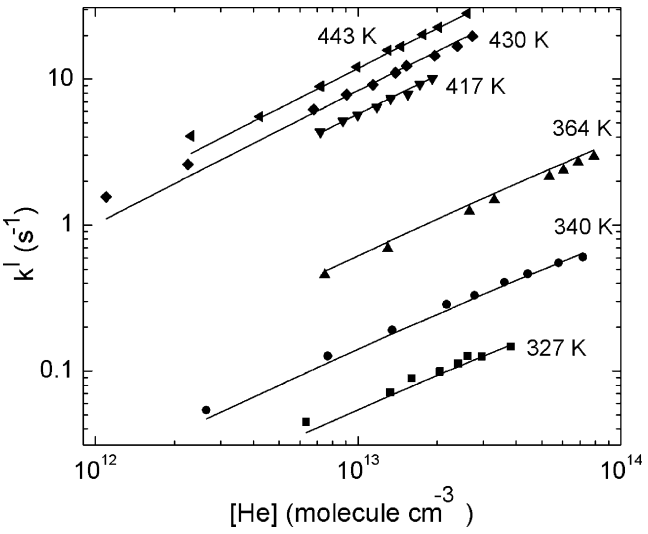

Fig. 3. First order rate coefficients for $HS_2O_7^-H_2SO_4$ cluster ion decomposition as a function of temperature and pressure. The solid lines are calculated with the master equation model for $E_0 = 25.1\,\text{kcal mol}^{-1}$ and $\beta = 1.16\,\text{kcal mol}^{-1}$.

A chi squared (χ^2) analysis was used to find the best fit of the master equation model to the experimental data.

$$\chi^2(E_0, \beta) = \sum_{T,P} \frac{(k^I_{\text{Model}}(E_0, \beta, T, P) - k^I_{\text{exp}}(T, P))^2}{\sigma^2} \quad (5)$$

where $k^I_{\text{exp}}(T, P)$ is the experimental first-order thermal decomposition rate constant at temperature T and pressure P, and $k^I_{\text{Model}}(E_0, \beta, T, P)$ is the first-order thermal decomposition rate constant calculated with the master equation model for bond energy E_0 and energy transfer parameter β. Chi-squared contours are plotted as a function of E_0 and β in Fig. 4. The minimum on the chi-squared surface gives the best fit bond energy and energy transfer parameter. It was assumed that the standard deviation (σ) of the measured rate constants was 10% of k^I_{exp}.

For the clusters $HS_2O_7^-(H_2SO_4)_x$ ($x = 2$ and 3), two decomposition channels were detected:

$$HS_2O_7^-(H_2SO_4)_x + He \rightarrow HSO_4^-(H_2SO_4)_x + SO_3 + He \quad (6)$$

$$HS_2O_7^-(H_2SO_4)_x + He \rightarrow HS_2O_7^-(H_2SO_4)_{x-1} + H_2SO_4 + He \quad (7)$$

In this case the master equation model was modified by expressing the unimolecular rate constant (Eq. (3)) as the sum of the unimolecular rate constants for two different channels

$$k_{\text{uni},i} = k_{\text{a,uni},i} + k_{\text{b,uni},i} \quad (8)$$

where $k_{\text{a,uni},i}$ and $k_{\text{b,uni},i}$ are the uni-molecular rate constants of reactant state i to decompose to channels a and b, respectively. The unimolecular rate constants were evaluated

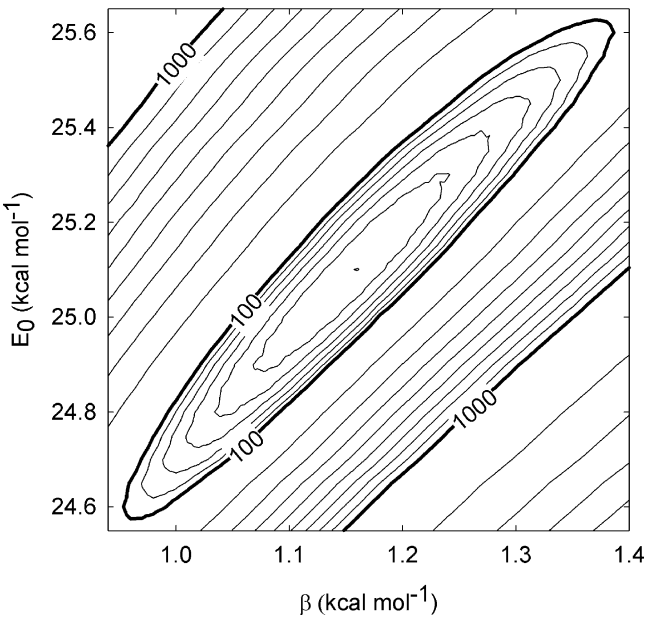

Fig. 4. Chi-squared contour plot of the master equation calculations for the $HS_2O_7^-H_2SO_4$ decomposition. The minimum chi-squared gives $E_0 = 25.1\,\text{kcal mol}^{-1}$ and $\beta = 1.16\,\text{kcal mol}^{-1}$.

as described previously [6] using the ab initio vibrational frequencies and rotational constants appropriate for the two channels.

The first-order thermal decomposition rate constants for each channel are averages of the unimolecular rate constants over the steady state distribution of the reactant:

$$k^I_{\text{a}} = \sum_i k_{\text{a,uni},i} f_{\text{ss},i} \quad (9)$$

$$k^I_{\text{b}} = \sum_i k_{\text{b,uni},i} f_{\text{ss},i} \quad (10)$$

where $f_{\text{ss},i}$ is the fractional steady state population of the reactant in state i. The branching ratios for each channel are then:

$$a = \frac{k^I_{\text{a}}}{k^I_{\text{a}} + k^I_{\text{b}}}, \qquad b = \frac{k^I_{\text{b}}}{k^I_{\text{a}} + k^I_{\text{b}}} \quad (11)$$

The branching between the two product channels is most sensitive to the bond energy difference between the two channels, which in this case is less than $1\,\text{kcal mol}^{-1}$. The two channel master equation has three input parameters: $E_{0\text{a}}$, $E_{0\text{b}}$ and β. The best-fit parameters were evaluated by minimizing chi-squared, as before.

The kinetics of the ligand switching reaction (1) were measured as a function of temperature. The rate constant for displacement of H_2SO_4 by SO_3 increased with temperature, suggesting that the reaction was endothermic as written. By assuming that the sum of the forward and reverse rate constants is equal to the collision rate constant [7], the reverse rate could be estimated. The equilibrium constant, given by the ratio of rate constants, was derived as a function of temperature. A van't Hoff plot of the temperature dependence

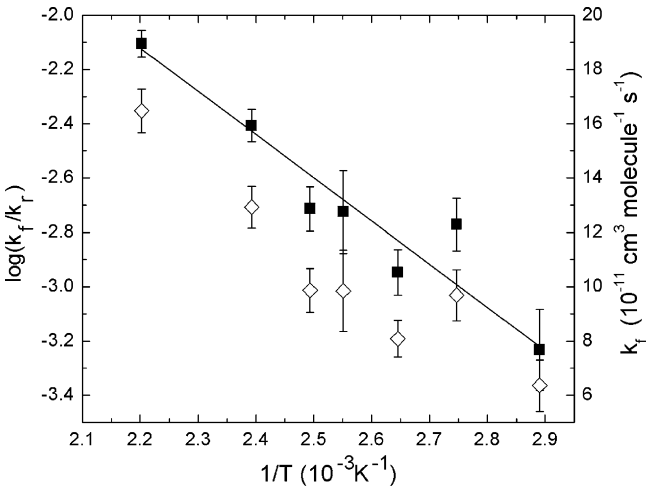

Fig. 5. Temperature dependence of the kinetics and equilibrium constant for $HSO_4^-(H_2SO_4)_2 + SO_3 \rightarrow HS_2O_7^-H_2SO_4 + H_2SO_4$. The solid squares are the logarithm of the equilibrium constant. The line is a fit to the data giving $\Delta H = 3.2\,\text{kcal mol}^{-1}$ and $\Delta S = 2.7\,\text{cal mol}^{-1}\,\text{K}^{-1}$ at $T_{ave} = 393\,\text{K}$. The open diamonds are the experimental rate constant for the forward reaction.

of the equilibrium constant is presented in Fig. 5. This analysis yields estimates for ΔH° and ΔS° for reaction (1).

2.4. Quantum chemistry calculations

ab initio calculations were performed at the HF/6-31+G (d) level of theory. Diffuse s and p shells were added to the second and third row atoms in order to improve the representation of the anion intermolecular hydrogen bonds [8]. The primary goal of the calculations was to determine the vibrational frequencies and the moments of inertia of the optimized molecular structures for use in the master equation analysis. Corrections for basis set superposition error [8,9] and electron correlation energies [8,10,11] were not performed. Vibrational frequencies were scaled by 0.89 [6,12,13] for the calculation of thermochemical properties and for use in the master equation model. All of the quantum chemical ab initio calculations were performed using the GAMESS software package [14] and the geometries were constructed and the GAMESS output was visualized with the MOLDEN software [15]. The geometry optimizations were performed with a maximum energy gradient tolerance of 1×10^{-5} hartree Bohr^{-1} or better.

3. Results and discussion

The experimental bond energies, ion/He energy transfer parameters and ab initio bond energies for the most stable structures are listed in Table 1. The master equation analysis is based on a reaction coordinate with no barriers and an orbiting transition state [6]. This should be valid for simple association/decomposition reactions involving hydrogen-bonded ligands (e.g., $H_2SO_4 + HSO_4^-(H_2SO_4)_x \leftrightarrow HSO_4^-(H_2SO_4)_{x+1}$). Arnold et al. report rate coefficients for the association reactions $SO_3 + HSO_4^-(H_2SO_4)_x \leftrightarrow HS_2O_7^-(H_2SO_4)_x$ that are close to the collision rate coefficient in 0.4 Torr He, showing that there are not significant barriers for these reactions [3]. The absolute error in the experimental bond energies is estimated to be about $1\,\text{kcal mol}^{-1}$ [6]. The experimentally derived bond energy is for most cases within $1.5\,\text{kcal mol}^{-1}$ of the ab initio calculated bond energy. For $HS_2O_7^-(H_2SO_4)_2$, the difference is about $3\,\text{kcal mol}^{-1}$.

Analysis of the temperature dependence of the forward reaction $HSO_4^-(H_2SO_4)_2 + SO_3 \rightarrow HS_2O_7^-H_2SO_4 + H_2SO_4$ yields an estimate for the reaction enthalpy. The van't Hoff plot shown in Fig. 5 gives $\Delta H^\circ_{393\,\text{K}} = 3.2\,\text{kcal mol}^{-1}$ and $\Delta S^\circ_{393\,\text{K}} = 2.7\,\text{kcal mol}^{-1}$ for the ligand switching reaction. An uncertainty of $2\,\text{kcal mol}^{-1}$ is assigned to the reaction enthalpy because it is based on the unsubstantiated assumption that the reverse reaction proceeds at the collision rate, and the measurement covers a relatively small range of temperature. The enthalpy change measured for the ligand switching reaction,

$$HSO_4^-(H_2SO_4)_2 + SO_3 \rightarrow HS_2O_7^-H_2SO_4 + H_2SO_4$$
$$\Delta H^\circ = 3.2 \pm 2.0\,\text{kcal mol}^{-1} \quad (12)$$

may be compared with values derived from measured bond enthalpies. Values listed in Eqs. (12)–(18) are evaluated for a temperature of 298 K. The reaction enthalpy for (12) may also be derived from the difference in the measured H_2SO_4 and SO_3 bond enthalpies in $HS_2O_7^-(H_2SO_4)_2$:

$$HSO_4^-(H_2SO_4)_2 + SO_3 \rightarrow HS_2O_7^-(H_2SO_4)_2$$
$$\Delta H^\circ = -23.0 \pm 1.0\,\text{kcal mol}^{-1} \quad (13)$$

$$HS_2O_7^-(H_2SO_4)_2 \rightarrow HS_2O_7^-H_2SO_4 + H_2SO_4,$$
$$\Delta H^\circ = 23.2 \pm 1.0\,\text{kcal mol}^{-1} \quad (14)$$

Table 1
Bond energies and energy transfer parameters derived from master equation analysis

Reactant cluster	Loss of SO_3			Loss of H_2SO_4		
	E_o (exp) (kcal mol^{-1})	β (kcal mol^{-1})	E_o (calc) (kcal mol^{-1})	E_o (exp) (kcal mol^{-1})	β (kcal mol^{-1})	E_o (calc) (kcal mol^{-1})
$HS_2O_7^-H_2SO_4$	25.1	1.16	25.8	Not observed		27.6
$HS_2O_7^-(H_2SO_4)_2$	22.8	1.00	19.5	23.4	1.00	20.6
$HS_2O_7^-(H_2SO_4)_3$	20.3	0.74	18.8	21.1	0.74	20.5

Table 2
Ab initio results for all geometries calculated

Isomer	E_{elec} (kcal mol^{-1})	E_{elec} (hartrees)	E_{ZP} (kcal mol^{-1})	$S^{\circ}_{298.15}$ (cal mol^{-1} K)
SO_3	−390303.98	−621.98846	7.65	61.28
H_2SO_4[a]	−438032.82	−698.04876	23.74	71.10
HSO_4^-[b]	−437717.14	−697.54607	16.50	71.90
$HS_2O_7^-$	−828062.17	−1319.59996	26.38	91.30
$HS_2O_7^-H_2SO_4$ (a)	−1266115.08	−2017.68111	51.19	128.69
$HS_2O_7^-H_2SO_4$ (b)	−1266118.09	−2017.68592	51.31	129.65
$HS_2O_7^-H_2SO_4$ (c)	−1266122.20	−2017.69247	51.45	131.70
$HS_2O_7^-H_2SO_4$ (d)	−1266123.96	−2017.69528	51.78	122.97
$HS_2O_7^-(H_2SO_4)_2$ (a)	−1704172.41	−2715.76933	76.57	161.88
$HS_2O_7^-(H_2SO_4)_2$ (b)	−1704172.79	−2715.76994	76.49	167.20
$HS_2O_7^-(H_2SO_4)_2$ (c)	−1704178.50	−2715.77904	76.84	158.12
$HS_2O_7^-(H_2SO_4)_3$ (a)	−2142232.78	−3413.86237	101.89	193.44
$HS_2O_7^-(H_2SO_4)_3$ (b)	−2142232.83	−3413.86245	101.83	198.40

E_{elec}: electronic energy. E_{ZP}: zero point energy.
[a] From [4]. Note error in S° reported in [4] has been corrected.
[b] From [4].

$$\text{net}: HSO_4^-(H_2SO_4)_2 + SO_3 \rightarrow HS_2O_7^-H_2SO_4 + H_2SO_4,$$
$$\text{net}: \Delta H^{\circ} = 0.2 \pm 1.4\,\text{kcal mol}^{-1} \quad (15)$$

The enthalpy of reaction (12) may also be derived from the difference between the H_2SO_4 binding in $HSO_4^-(H_2SO_4)_2$ [6] and the SO_3 binding in $HS_2O_7^-H_2SO_4$

$$HSO_4^-H_2SO_4 + SO_3 \rightarrow HS_2O_7^-H_2SO_4,$$
$$\Delta H^{\circ} = -25.3 \pm 1.0\,\text{kcal mol}^{-1} \quad (16)$$

$$HSO_4^-(H_2SO_4)_2 \rightarrow HSO_4^-H_2SO_4 + H_2SO_4,$$
$$\Delta H^{\circ} = 27.4 \pm 1.0\,\text{kcal mol}^{-1} \quad (17)$$

$$\text{net}: HSO_4^-(H_2SO_4)_2 + SO_3 \rightarrow HS_2O_7^-H_2SO_4 + H_2SO_4,$$
$$\text{net}: \Delta H^{\circ} = 2.1 \pm 1.4\,\text{kcal mol}^{-1} \quad (18)$$

This comparison shows that the results agree within the estimated error. A weighted average value of the three results is: $\Delta H^{\circ} = 1.6 \pm 0.9\,\text{kcal mol}^{-1}$. Applying similar thermodynamic cycles one derives reaction enthalpies for $HSO_4^-(H_2SO_4)_x + SO_3 \rightarrow (H_2SO_4)_{x-1} + H_2SO_4$ of $\Delta H^{\circ}_{298\,K} = 2.3 \pm 1.0\,\text{kcal mol}^{-1}$, $\Delta H^{\circ}_{298\,K} = 0.6 \pm 1.0\,\text{kcal mol}^{-1}$ and $\Delta H^{\circ}_{298\,K} = 1.3 \pm 1.4\,\text{kcal mol}^{-1}$, for $x = 1$, 3 and 4 respectively.

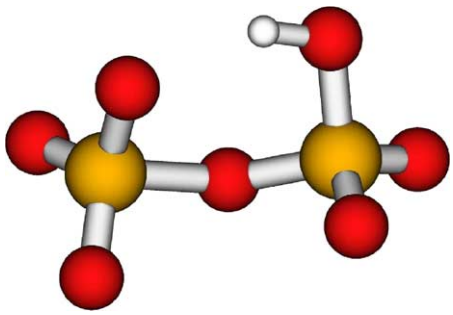

Fig. 6. Structure of $HS_2O_7^-$.

The ab initio results for all the measured cluster ions and their isomers are listed in Table 2. The geometries of the calculated clusters are shown in Figs. 6–9, molecular structures, moments of inertia, and vibrational frequencies are

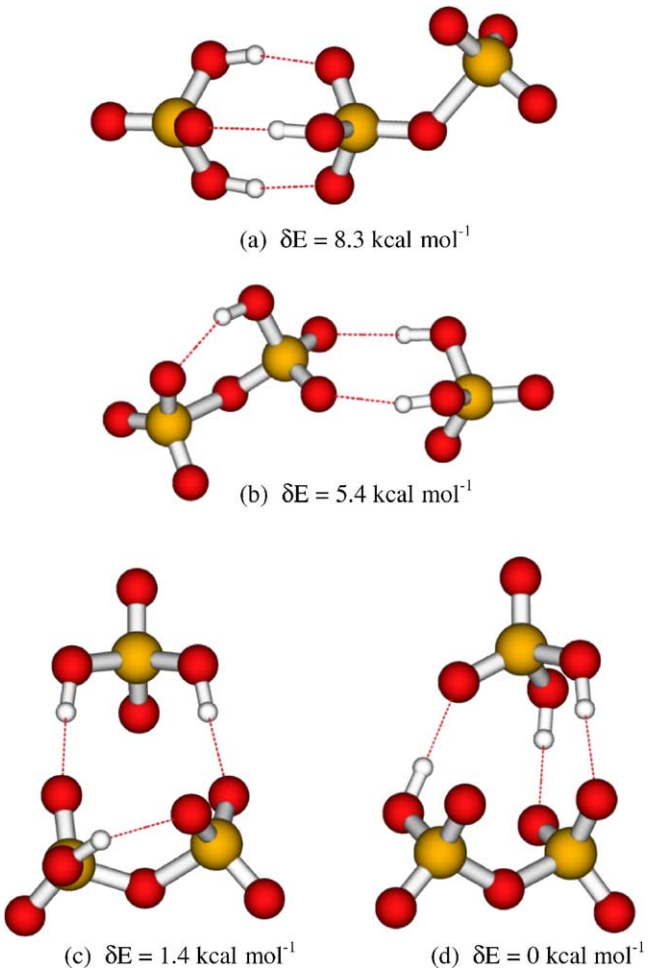

Fig. 7. Structure of $HS_2O_7^-H_2SO_4$. δE is the difference in the total energy, $E_{tot} = E_{elec} + E_{ZP}$, relative to the most stable isomer.

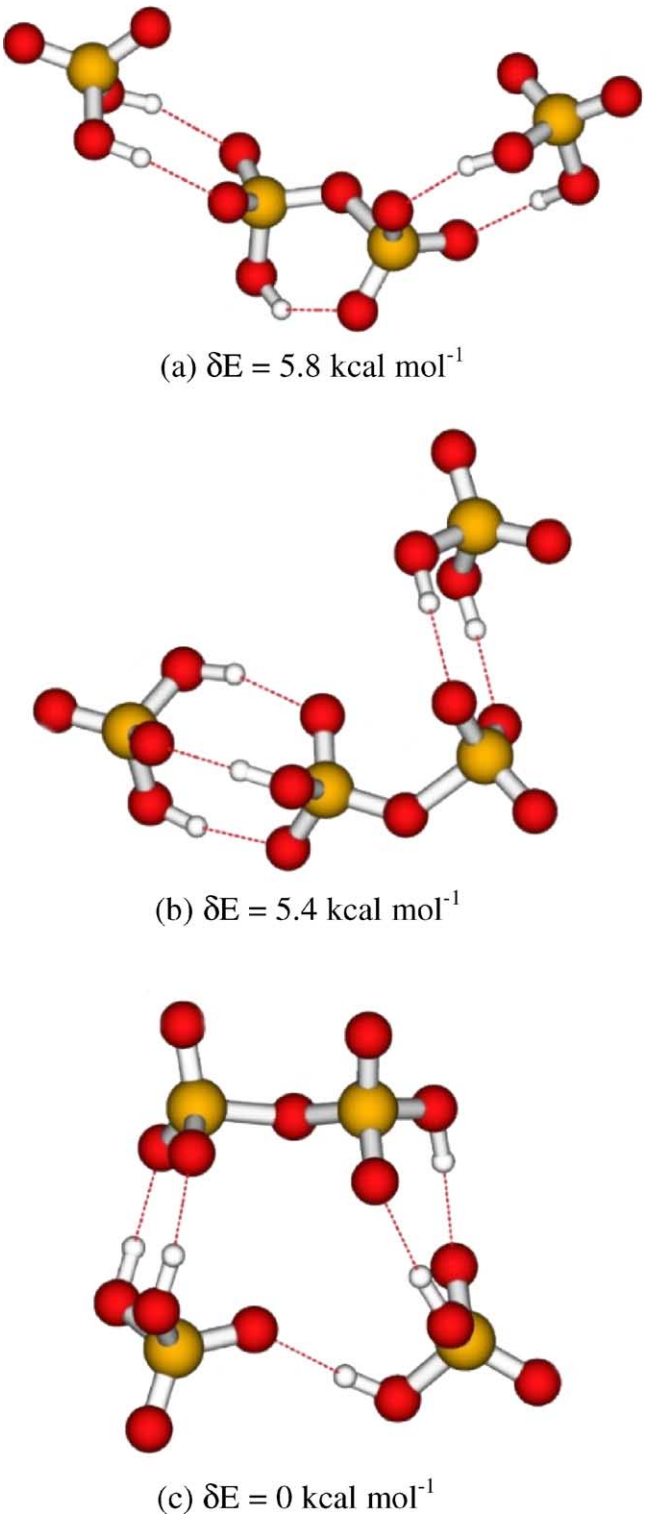

Fig. 8. Structure of $HS_2O_7^-(H_2SO_4)_2$. δE is the difference in the total energy, $E_{tot} = E_{elec} + E_{ZP}$, relative to the most stable isomer.

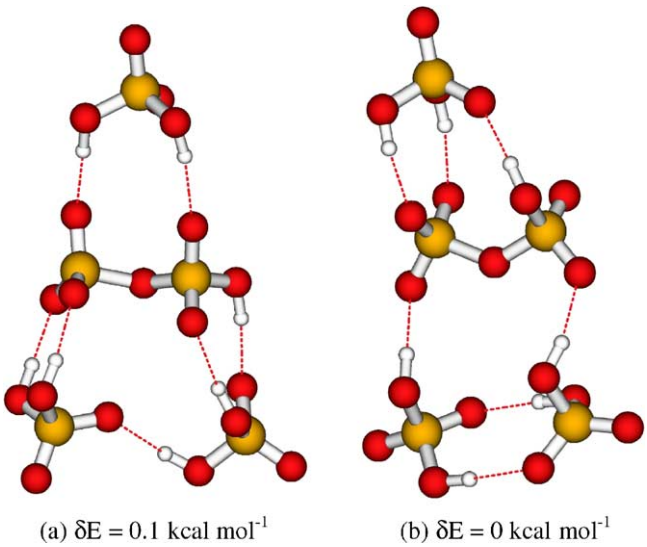

Fig. 9. Structure of $HS_2O_7^-(H_2SO_4)_3$. δE is the difference in the total energy, $E_{tot} = E_{elec} + E_{ZP}$, relative to the most stable isomer.

available as Supplementary Information. The results of the ab initio calculations show that the core ion in these clusters is $HS_2O_7^-$, the negative ion of pyrosulfuric acid. Four structures of $HS_2O_7^-H_2SO_4$ were calculated. The cyclic structure with H_2SO_4 forming three favorable hydrogen bonds to $HS_2O_7^-$ is the lowest in energy. The linear structures 7 (a) and (b) have the highest energies. The next larger cluster $HS_2O_7^-(H_2SO_4)_2$ shows the same trend. The cyclic structure, Fig. 8(c), with the core ion $HS_2O_7^-$ and one H-bond between neutral H_2SO_4 ligands has the lowest electronic energy and entropy. Two nearly degenerate cyclic isomers of $HS_2O_7^-(H_2SO_4)_3$ are shown in Fig. 9. Structure 9(a) is generated by adding one H_2SO_4 to the most stable $HS_2O_7^-(H_2SO_4)_2$ isomer (Fig. 8(c)), and 9(b) is constructed by bridging two H_2SO_4 molecules across $HS_2O_7^-$ in the most stable $HS_2O_7^-H_2SO_4$ structure (Fig. 7(d)).

A comparison of the experimentally derived bond energies of SO_3 and H_2SO_4 to the $HSO_4^-(H_2SO_4)_x$ cluster ions [6], shows that H_2SO_4 is only bonded 2.5, 1.2 and 1.5 kcal mol^{-1} stronger than SO_3 for $x = 1$, 2 and 3, respectively. Reaction enthalpies for $HS_2O_7^-(H_2SO_4)_x + H_2O \rightarrow HSO_4^-(H_2SO_4)_{x+1}$ may be derived from a combination of the thermodynamic data reported in the present study and previous work [4]. For example, the experimental reaction enthalpy for the neutral reaction [16]

$$SO_3 + H_2O \rightarrow H_2SO_4, \quad \Delta H^\circ_{298K} = -23.3\,\text{kcal mol}^{-1} \tag{19}$$

combined with

$$HS_2O_7^-H_2SO_4 + H_2SO_4 \rightarrow HSO_4^-(H_2SO_4)_2 + SO_3, \quad \Delta H^\circ_{298\,K} = -1.6\,\text{kcal mol}^{-1} \tag{20}$$

gives the net reaction

$$HS_2O_7^-H_2SO_4 + H_2O \rightarrow HSO_4^-(H_2SO_4)_2, \quad \text{net}: \Delta H^\circ_{298\,K} = -24.9\,\text{kcal mol}^{-1} \tag{21}$$

Similar logic applied to the reactions $HS_2O_7^-(H_2SO_4)_x + H_2O \rightarrow HSO_4^-(H_2SO_4)_{x+1}$ ($x = 0, 1, 2, 3$) yields reaction enthalpies of -25.0, -24.9, -23.9 and $-24.6\,kcal\,mol^{-1}$, for $x = 0, 1, 2, 3$ respectively. Curtius et al. [4] did not observe the elimination of H_2O from $HSO_4^-(H_2SO_4)_y$ thermal decomposition, even though for $y = 1$ and 2, H_2O elimination appears to be the lowest energy path. This may suggest that there is a significant barrier to H_2O elimination from H_2SO_4 in these clusters, similar to that observed in free H_2SO_4 (reaction 19) [17].

4. Summary

The temperature and pressure dependence for the thermal decomposition of $HS_2O_7^-(H_2SO_4)_x$ ($x = 1$–3) were measured in a quadrupole ion trap. Bond energies were derived from the decomposition kinetics using a master equation model. The SO_3 bonding to the $HSO_4^-(H_2SO_4)_x$ ($x = 1, 2, 3$) ions is strong and only slightly weaker than that of sulfuric acid to the same cluster ions. The ligand switching reaction $HSO_4^-(H_2SO_4)_2 + SO_3 \rightarrow HS_2O_7^-(H_2SO_4)_1 + H_2SO_4$ was also studied as a function of pressure and temperature. Ab initio calculations yield information on the structures, vibrational frequencies, moments of inertia and entropies of these clusters. The ab initio calculations show that SO_3 reacts with $HSO_4^-(H_2SO_4)_x$ ions to produce cluster ions based on the $HS_2O_7^-$ ion rather than HSO_4^-. Ab initio bond energies agree, in most of the cases, within $1.5\,kcal\,mol^{-1}$ of the experimental results. A detailed analysis of stratospheric SO_3 concentration based on our results is beyond the scope of the paper and will be presented in a separate publication.

Acknowledgements

We thank the NOAA Forecast Systems Lab for use of computer time on the JET computer cluster facility. The work was supported in part by NOAA's Climate and Global Change Program.

References

[1] H. Schlager, F. Arnold, Planet. Space Sci. 25 (1987) 693.
[2] T. Reiner, F. Arnold, Geophys. Res. Lett. 24 (1997) 1751.
[3] S.T. Arnold, R.A. Morris, A.A. Viggiano, J.T. Jayne, J. Geophys. Res. 100 (1995) 14 141.
[4] J. Curtius, K.D. Froyd, E.R. Lovejoy, J. Phys. Chem. A 105 (2001) 10867.
[5] See, for example: L. Chen, T.C.L. Wang, T.L. Ricca, A.G. Marshall, Anal. Chem. 59 (1987) 449.;
M. Soni, R.G. Cooks, Anal. Chem. 66 (1994) 2488;
D.E. Goeringer, K.G. Asano, S.A. McLuckey, D. Hoekman, S.W. Stiller, Anal. Chem. 66 (1994) 313.
[6] E.R. Lovejoy, J. Curtius, J. Phys. Chem. A 105 (2001) 10874.
[7] T. Su, W.J. Chesnavich, J. Chem. Phys. 76 (1982) 5183.
[8] E.R. Davidson, D. Feller, Chem. Rev. 86 (1986) 681.
[9] S. Simon, M. Duran, J.J. Dannenberg, J. Phys. Chem. A 103 (1999) 1640.
[10] M. Head-Gordon, J. Phys. Chem. 100 (1996) 13213.
[11] K. Raghavachari, J.B. Anderson, J. Phys. Chem. 100 (1996) 12960.
[12] E.R. Lovejoy, R. Bianco, J. Phys. Chem. A 104 (2000) 10280.
[13] A.P. Scott, L. Radom, J. Chem. Phys. 100 (1996) 16502.
[14] M.W. Schmidt, K.K. Baldridge, J.A. Boatz, S.T. Elbert, M.S. Gordon, J.H. Jensen, S. Koseki, N. Matsunaga, K.A. Nguyen, S. Su, T.L. Windus, M. Dupuis, J.A. Montgomery, J. Comput. Chem. 14 (1993) 1347.
[15] G. Schaftenaar, J.H. Noordik, J. Comput.-Aided Mol. Design 14 (2000) 123.
[16] M.W. Chase, Jr., C.A. Davies, J.R. Downey, Jr., D.J. Frurip, R.A. McDonald, A.N. Syverud, JANAF Thermochemical Tables J. Phys. Chem. Ref. Data. 14 (1) (1984).
[17] K. Morokuma, C. Muguruma, J. Am. Chem. Soc. 116 (1994) 10316.